Real-time indoor positioning system for a smart workshop using white LEDs and a phase-difference-of-arrival approach

Du, Pengfei; Zhang, Sheng; Zhong, Wen-De; Chen, Chen; Yang, Helin; Alphones, Arokiaswami; Zhang, Ran

2019

Du, P., Zhang, S., Zhong, W.-D., Chen, C., Yang, H., Alphones, A., & Zhang, R. (2019). Real-time indoor positioning system for a smart workshop using white LEDs and a phase-difference-of-arrival approach. Optical Engineering, 58(8), 084112-. doi:10.1117/1.oe.58.8.084112

https://hdl.handle.net/10356/141896

https://doi.org/10.1117/1.OE.58.8.084112

Real-time indoor positioning system for a smart workshop using white LEDs and a phase-difference-of-arrival approach

Pengfei Du,[a,b,*] Sheng Zhang,[a] Wen-De Zhong,[a] Chen Chen,[c] Helin Yang,[a] Arokiaswami Alphones,[a] and Ran Zhang[a]
[a]Nanyang Technological University, School of Electrical and Electronic Engineering, Singapore
[b]A*STAR's Singapore Institute of Manufacturing Technology, Innovis, Singapore
[c]Chongqing University, School of Microelectronics and Communication Engineering, Chongqing, China

Abstract. In order to provide a cost-effective indoor positioning and tracking service for autonomous ground vehicles and other important assets in smart factories, we report the theory and experiments for a real-time indoor positioning system using commercially available LED lamps. Inspired by the fundamental theory of the global navigation satellite system, the proposed system uses the phase difference of arrival (PDOA) approach to obtain the time difference of arrival of each carrier transmitted from individual modified LED lamps so as to estimate the receiver position. A prototype of the atto-cellular positioning system covering an area of 2.2×1.8 m^2 with a height of 2 m was designed and experimentally demonstrated. For the design, we performed a simulation based on the Crámer–Rao bound to achieve optimal LED lamp arrangement, RF power, and other parameters. Furthermore, a virtual local oscillator for the PDOA scheme was applied to reduce the hardware complexity and to ensure the processing speed. In the experiment, the receiver was mounted on a movable material buffer station in a smart workshop, and the positioning performance was validated by tracking the trajectory of the material buffer station moving within the positioning coverage area. The experimental results show that an average positioning accuracy of ~7 cm was achieved.
[DOI: 10.1117/1.OE.58.8.084112]

Keywords: visible light communication; visible light positioning; phase-difference-of-arrival; light-emitting diode; light-fidelity.

Paper 190594 received May 8, 2019; accepted for publication Aug. 7, 2019; published online Aug. 30, 2019.

1 Introduction

The concept of the smart factory or manufacturing on demand under the framework of the internet of things (IOT) has become increasingly popular in recent years. As one of the pillars of the smart factory and IOT, indoor positioning technology enables automatic guided vehicles (AGVs), important assets, and even the containers for inventory with full location awareness.[1,2] Before the emergence of indoor visible light positioning (VLP) service based on visible light communication,[3] or light-fidelity (Li-Fi),[4,5] a number of conventional RF-based indoor positioning technologies were applied in smart factories, but they inevitably suffered from strong interference and high cost.[2,6,7] Recently, VLP has become increasingly attractive because of the ubiquitous adoption of LED lighting infrastructure.[6–8] Indoor VLP service is superior to conventional techniques such as Wi-Fi and ultra-wideband (UWB) in terms of accuracy, interference-free spectrum, and infrastructure deployment. In particular, VLP's line-of-sight transmission avoids the severe multipath effect that limits the achievable accuracy of positioning using Wi-Fi and UWB. Several positioning methods, such as received-signal-strength schemes,[9] angle-of-arrival approaches[10,11] or imaging-sensor-based methods,[12] and time-of-arrival (TOA) methods or time-difference-of-arrival (TDOA) approaches[13,14] have been adopted by VLP researchers. Among those various means, the TDOA method shows the highest accuracy and robustness with similar hardware complexity and costs.[15,16]

In 2018, we experimentally realized VLP using TDOA through digital usage of a virtual local oscillator (VLO).[17] Despite the reduction in complexity afforded by the VLO and interpolation technique, the TDOA method is based on cross-correlation, and thus always relies heavily on digitization with a high sampling rate.[18] To avoid the cross-correlation-based TDOA approach, we further proposed and validated an alternative TDOA scheme based on phase-difference-of-arrival (PDOA) measurement.[19] It uses an extra-carrier signal in one of the LED transmitters so as to avoid the usage of local signals. However, this solution sacrifices the ease of deployment and increases the algorithm complexity.

To address these issues, this study was conducted to theoretically and experimentally develop a real-time two-dimensional (2-D) indoor positioning system, using commercially available LED lamps, which uses PDOA to calculate TDOA from carrier signals transmitted from the LED lamps to complete localization tasks. Through digital usage of VLO,[17] the proposed system further benefits from reduced implementation complexity. To further enhance system performance, some configuration parameters were theoretically optimized by evaluating Crámer–Rao bounds. The proposed system was realized and verified experimentally in a smart workshop. The average positioning accuracy of the VLP system utilizing the proposed scheme is less than 10 cm in a coverage area of 2.2×1.8 m^2. The research progress is believed to have a potential impact on the implementation of Li-Fi and indoor positioning using white LEDs, which has always been

*Address all correspondence to Pengfei Du, E-mail: pfdu@ntu.edu.sg

0091-3286/2019/$28.00 © 2019 SPIE

attractive to researchers in the area of smart factories and optical IOT. The main contributions of our work are:

- The proposed application of VLO in a VLP system using PDOA in order to reduce system complexity.
- The method for optimizing LED lamp arrangement, RF power, and other configuration parameters using Crámer–Rao bound derivation.
- The experimental verification of the performance of the proposed scheme in a smart workshop.

The rest of this paper is organized as follows. In Sec. 2, the proposed VLP scheme is presented, ranging from the systematic overview to the PDOA algorithm with the VLO technique. Section 3 discusses the theoretical boundaries based on the numerical simulations. Section 4 describes the demonstration of the positioning system prototype and its experimental validation in terms of accuracy. Finally, a summary of the conclusions is discussed in Sec. 5.

2 Principle

This section provides an overview of the VLP system and elaborates the proposed scheme of PDOA-based position estimation, particularly including phase-of-arrival (POA) measurement with virtual local signals.

2.1 *Overview of the PDOA-Based VLP System*

Inspired by the fundamental theory of the global navigation satellite system (GNSS), the proposed system uses PDOA approach to measure the TDOA of any two carriers transmitted from individual modified LED lamps so as to estimate the receiver position. Likewise, the three LED lamps are considered as three "indoor satellites," as shown in Fig. 1, which broadcast the synchronized carriers so that the users can receive all the carriers and measure TDOA values from PDOA to determine their own locations. As shown in Fig. 1, the VLP system has a cellular form at the transmitter side to achieve greater coverage, in which three neighboring LED lamps are grouped into one atto-cellular unit.[20] It is noteworthy that the performance of the VLP system can be roughly represented by one atto-cell unit. Hence, we preliminarily concentrated on the performance of one atto-cell unit in this study without loss of generality. As shown in Fig. 1, the signal generator generates sinusoidal waves with unique frequencies as modulation signals for every LED transmitter. The current boosters amplify the modulated signals, and the bias tees subsequently combine them with DC power for simultaneous illumination. The bottom of Fig. 1 shows the VLP receiver for users, consisting of an avalanche photodetector coupled with an optical blue filter and a digital localization module. The digital localization module consists of a digitizer, a PDOA measuring module, and a position estimator. The digitizer first converts the analog output of the photodetector into digital signals. The PDOA measuring module subsequently calculates the TDOA from LED transmitters based on POA measurement according to the proposed algorithm introduced in the next section.

2.2 *PDOA Algorithm*

The essence of the PDOA algorithm is to indirectly achieve the TDOA from phase measurement. Although the algorithm is labeled by PDOA,[15] there is no actual PDOA value involved. A schematic of the PDOA algorithm is shown in Fig. 2. After digitization, the originally received signal is split by predetermined bandpass filters (see BPF #1-3 in Fig. 2) into the carrier signals of different frequencies generated by several LED transmitters. Then, the carrier signal is sent to the sync cutter. Meanwhile, the filtered carrier is also pumped into a peak detector, which provides the location of the first peak of the originally received signal in units of sample points. The procedure of the peak detector is: (1) it initially mixes all the carrier signals into a mixed sinewave after normalization; and (2) it then finds the maximum absolute value within the first common period. The sync cutter of each carrier channel truncates a certain amount of sample points of the collected data as per the result provided by the peak detector. Once the truncation is completed by the sync cutter, the truncated signal is transferred to the multiplier, yielding the product of the truncated signal and the local signal. The local signal is sourced from the VLO, which is digitally built in the software. At the end, a low-pass filter (LPF) for each carrier channel removes the high-frequency components and retains the DC components containing ϕ_i', which represents the relative phase difference between the carrier signal from

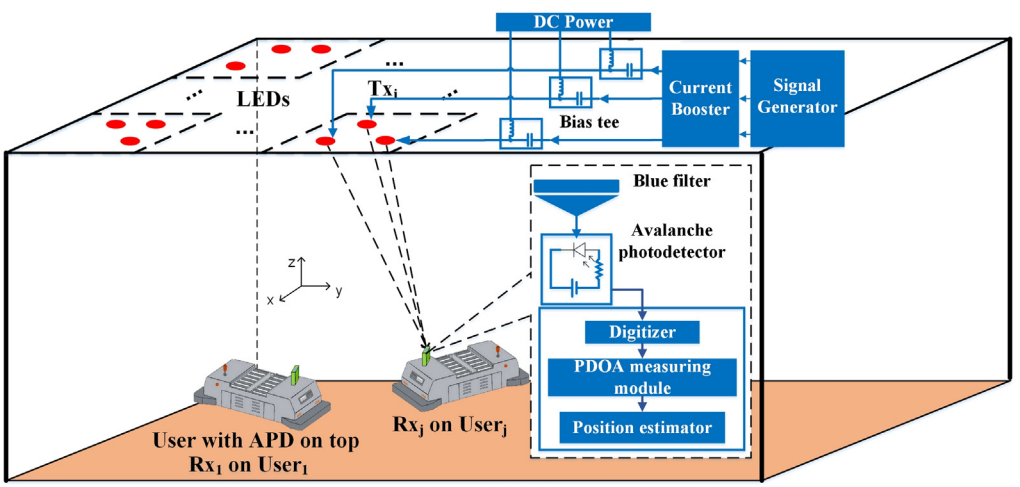

Fig. 1 Schematic of the atto-cellular VLP system in a workshop.

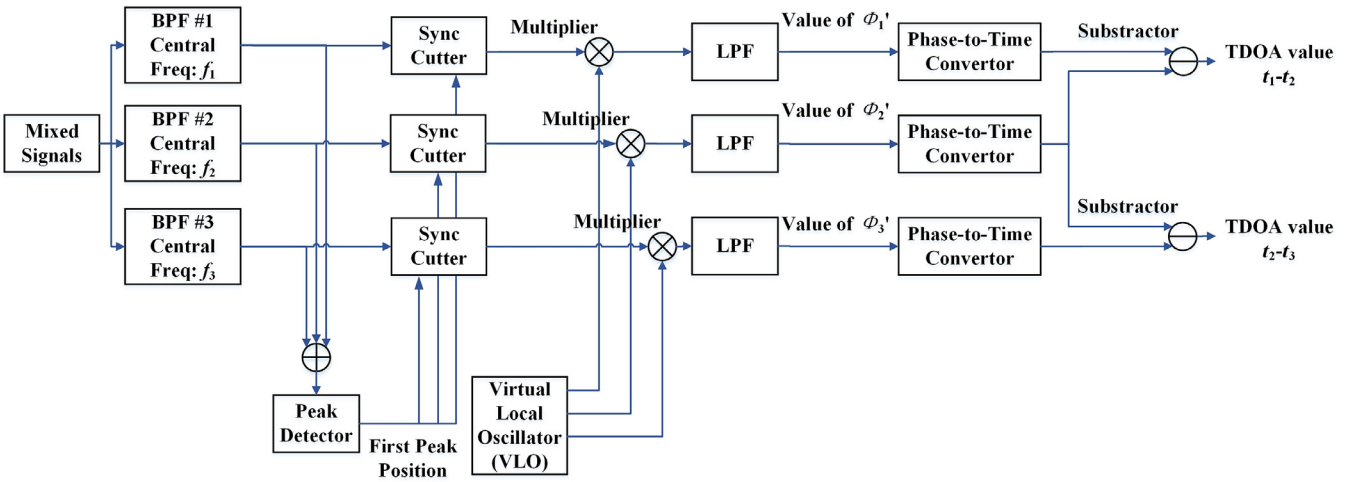

Fig. 2 Schematic of the PDOA algorithm.

the i'th LED and the virtual local signal with the same frequency. Considering the PDOA-based VLP as a quasi-synchronized system,[8] ϕ_i' includes not only the POA ϕ_i from the i'th LED to the receiver but also the unknown initial time difference between the carrier and the local signal denoted by t_{PR}. Hence, the relationship is formulated as

$$\phi_i' = \phi_i + (t_{PR} \cdot 2\pi f_i), \tag{1}$$

where f_i denotes the carrier frequency transmitted by the i'th LED. t_{PR} is equivalent to the pure pseudorange (PR) in the GNSS technique.[21] Likewise, t_{PR} is expected to be the same for all the output of LPFs, because the carriers of all LEDs are synchronized to each other. Hence, t_{PR} can be offset by calculating the TDOA by subtraction.[21] Unlike the approach employing a real local oscillating signal, using a virtual local signal demands an additional time constraint. In other words, t_{PR} is the same for all the LPF outputs only when the time interval between data acquisitions in each measurement is a multiple of the common period shared by all carriers.[17] That is also the motivation for deploying the sync cutter and peak detector. Finally, the output of each subtractor shown in Fig. 2 is converted into TDOA, denoted by $t_1 - t_2$ and $t_2 - t_3$, respectively.

Eventually, the position is determined by the position estimator as shown in Fig. 1 based on the TDOA values translated from POA values and the trilateration method. Let (x_i, y_i, z_i) be the coordinates of the i'th LED, c be the speed of light, and (X_r, Y_r, Z_r) be the coordinates of the receiver. We have

$$\begin{cases} \sqrt{(x_1 - X_r)^2 + (y_1 - Y_r)^2 + (z_1 - Z_r)^2} - \sqrt{(x_2 - X_r)^2 + (y_2 - Y_r)^2 + (z_2 - Z_r)^2} = c \cdot \left(\frac{\phi_1'}{2\pi f_1} - \frac{\phi_2'}{2\pi f_2}\right) \\ \sqrt{(x_2 - X_r)^2 + (y_2 - Y_r)^2 + (z_2 - Z_r)^2} - \sqrt{(x_3 - X_r)^2 + (y_3 - Y_r)^2 + (z_3 - Z_r)^2} = c \cdot \left(\frac{\phi_2'}{2\pi f_2} - \frac{\phi_3'}{2\pi f_3}\right). \end{cases} \tag{2}$$

To solve Eq. (2) and hence to acquire the desired coordinates (X_r, Y_r, Z_r), numerical methods, such as Newton–Raphson and Levenberg–Marquard, are generally used.[22]

3 Theoretical Boundaries

This section discusses the theoretical boundaries derived from simulations. The optimal configuration was also determined according to the simulation works.

3.1 *Crámer–Rao Bound Derivation*

For simplicity and without loss of generality, the scenario of 2-D positioning was specifically considered, and the process of the POA/TOA and PDOA/TDOA was assumed as an unbiased estimation. Theoretically, the Crámer–Rao lower bound (CRLB) of PDOA estimation can be given through a Fisher matrix[23,24] but not easily in the closed form; this is not convenient for optimization of system deployment. Hence, an approximated closed form of CRLB of PDOA estimation was utilized in this study on the basis of existing research.[25,26] First, the CRLB of POA estimation at the j'th position from the i'th LED transmitter is given in the literature as[25,26]

$$\sigma^2_{\mathrm{POA}_{i,j}} = \frac{c^2}{(2\pi\sqrt{3}f_c)^2 \cdot t_s \cdot \sqrt{3}f_c \cdot \mathrm{SNR}_{i,j}} = \frac{c^2}{(2\pi\sqrt{3}f_c)^2 \cdot t_s \cdot \sqrt{3}f_c \cdot (Ex \cdot At_{i,j}^2 \cdot Rp^2)/N_0}, \tag{3}$$

where f_c is the carrier frequency and t_s is the duration of the signal for processing. As is commonly known, the signal-to-noise ratio (SNR) at the j'th position from i'th LED transmitter can be rewritten as a function of photodetector responsivity with gain Rp, RF power Ex, noise power N_0, and channel attenuation $At_{i,j}$ at the j'th position from the i'th LED transmitter. Therefore, CRLB for PDOA at j'th position is derived as

$$\sigma^2_{\mathrm{PDOA}_j} < \max[\sigma^2_{\mathrm{POA}_{1,j}} + \sigma^2_{\mathrm{POA}_{2,j}}\sigma^2_{\mathrm{POA}_{2,j}} + \sigma^2_{\mathrm{POA}_{3,j}}]. \tag{4}$$

If the SNR is sufficiently high in a certain range, Eq. (4) can be rewritten as

$$\sigma^2_{\mathrm{PDOA}_j} \approx \max\left[\sum_{i=1}^{2}\frac{c^2}{(2\pi\sqrt{3}f_c)^2\cdot t_s\cdot\sqrt{3}f_c\cdot(Ex\cdot At_{i,j}^2\cdot Rp^2)/N_0}, \sum_{i=2}^{3}\frac{c^2}{(2\pi\sqrt{3}f_c)^2\cdot t_s\cdot\sqrt{3}f_c\cdot(Ex\cdot At_{i,j}^2\cdot Rp^2)/N_0}\right]. \tag{5}$$

In Eq. (5), the noise power N_0 and channel attenuation $At_{i,j}$ can be expressed as

$$At_{i,j} = \frac{m+1}{2\pi\cdot d_{i,j}^2}\cdot Ar\cdot\cos^2(\psi_{i,j})\cdot\cos(\theta)\cdot\alpha\cdot\eta, \tag{6}$$

$$N_0 = 2q\cdot B\cdot(\gamma\cdot P_{\mathrm{opt}} + I_{bg}\cdot I_B) + \left(\frac{8\pi\cdot k\cdot Tk\cdot Ar\cdot I_B\cdot Cap\cdot B^2}{Gol}\right) + \left(\frac{16\pi^2\cdot k\cdot Tk\cdot\tau\cdot Ar^2\cdot I_3\cdot Cap^2\cdot B^3}{gm}\right). \tag{7}$$

In Eqs. (6) and (7), $d_{i,j}$ is the distance between the receiver at the j'th position and the i'th LED transmitter; Ar is the area of the photodetector (20 mm^2); m is the Lambertian order of the LED transmitter; $\psi_{i,j}$ is the irradiation angle of the i'th LED with respect to the receiver at the j'th position; θ denotes the incidence angle; α represents the efficiency of the blue filter; η is the transmittance of window glass; Gol is the open-loop gain of the photodetector, set as 1767.578 V/A herein; and γ is the responsivity of the photodetector, set as 16.54 A/W herein. Elsewhere, P_{opt} is the power of the incident light; q is the electronics charge (1.6×10^{-19} C); I_{bg} is the background current, set as 5.10001×10^{-3} A; I_B and I_3 are the noise bandwidth factor (0.562 and 0.0868 Hz^{-1}); k is Boltzmann's constant (1.38064852×10^{-23} m^{2}kg s^{-2}K^{-1}); Tk is the environmental temperature in Kelvin (298.15 K); gm is the transconductance of the field effect transistor (FET) (30×10^{-3} S); τ is the FET channel noise factor, set as 1.5 herein; Cap is the fixed capacitance of the photodetector, set as 112×10^{-8} F herein; and B is the equivalent noise bandwidth, normally assumed as 20 MHz.

3.2 *Simulation Results and Discussion*

Using the derived CRLB model, we investigated some important configuration parameters, including the carrier frequencies, RF power, coverage, and LED arrangements. Both the 95% cumulative distribution function (CDF) error and average error were adopted as metrics to quantify the CRLB and hence to evaluate the configuration parameters. Figure 3 shows the CRLB curves versus different carrier frequencies, RF power, coverage, and LED arrangements. First, the carrier frequency was studied in a coverage area of 4 m × 4 m. As shown in Fig. 3(a), the curve becomes flat after the carrier frequency exceeds 4 MHz, so we opted for 4 MHz as the optimal carrier frequency. Then, we investigated the CRLB versus coverage under a carrier frequency of 4 MHz. In Fig. 3(b), a dramatic increase in positioning error is observed when the coverage exceeds 3 m × 3 m, hence a reasonable coverage area was chosen as 3 m × 3 m. Likewise, the RF power and LED arrangements were also optimized sequentially. Investigating the optimal LED arrangement is an important theoretical work because using

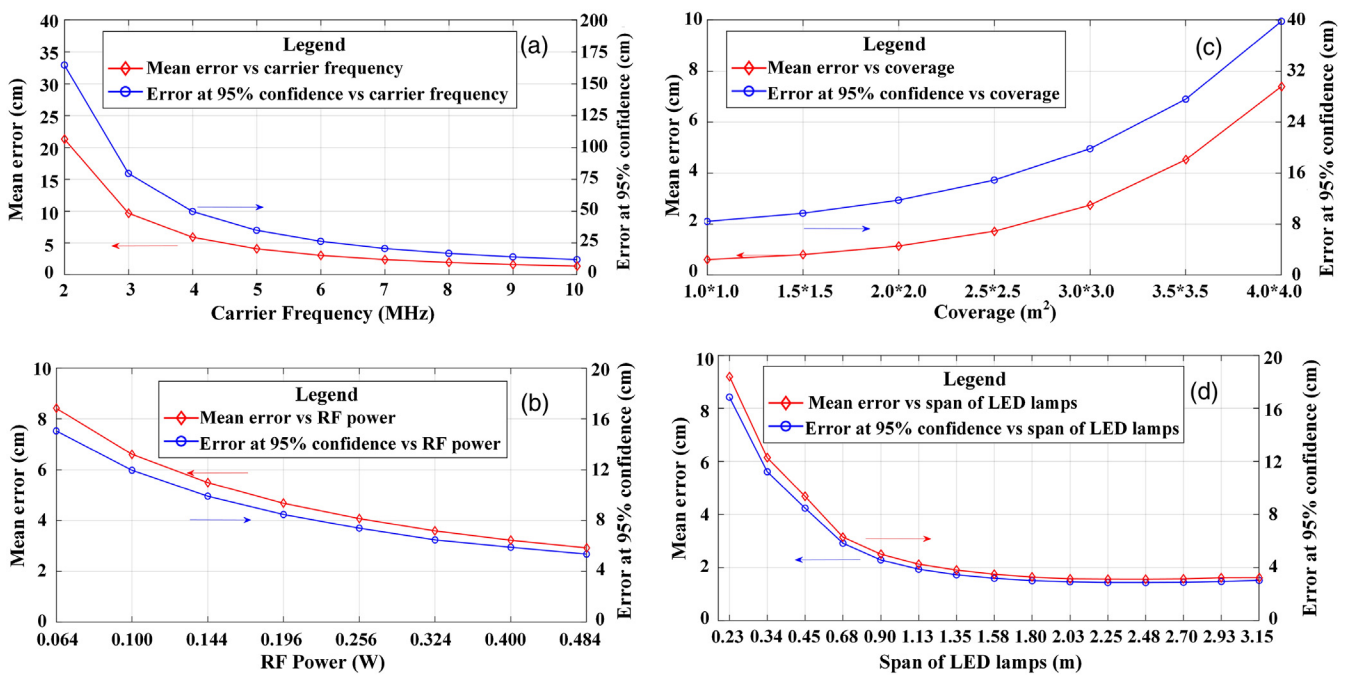

Fig. 3 Theoretical bound of VLP under different (a) carrier frequencies, (b) RF power, (c) coverage, and (d) span of LED lamps.

optimal LED arrangement can not only increase the positioning accuracy[15] but also improve the coverage area.[27] It is noteworthy that the LED arrangements herein were confined in equilateral triangles only, because this has been identified as the most suitable arrangement.[15] Thus, we needed only to find the optimal span of the LED lamps (i.e., the length of one side of the equilateral triangle). It should be also noted that the nonlinearity effect impacts the performance when adjusting the RF power and that the nonuniform initial time delay at different irradiation angles affects performance when adjusting the span of two individual LED lamps, both of which are neglected in the current CRLB model. Therefore, the previous works[15,19] offer us some guidelines to thoroughly consider the optimal values by combining the results from Figs. 3(c) and 3(d).

The optimal parameters based on the theoretical analysis are concluded as the following: the optimal carrier frequency is 4 MHz, the reasonable maximum coverage is 3 m × 3 m, the optimal RF power for each LED lamp is 0.196 to 0.2 W, and the optimal span of two individual LED lamps should be greater than 0.4 m in a single VLP unit. Furthermore, it is concluded that the theoretical accuracy boundary for an optimal VLP unit using 4 MHz carrier frequency is 10 cm at 95% confidence in a coverage area of 3 m × 3 m.

4 Experimental Demonstration

4.1 *Atto-Cell VLP Unit Prototype*

The prototype atto-cell VLP unit for experimental investigation was realized with the optimal parameters described in Sec. 3.2. Figure 4 shows a photograph of the experimental setup. Three LED lamps (Lumiled LXK8-PW50-0206) were the transmitters, mounted on the ceiling at a height of 2 m. Allocated to LED#1, LED#2, and LED#3 were the RF carrier frequencies of 4, 4.2, and 4.4 MHz, respectively. The synchronized RF carriers were generated by a signal generator (Spectrum M4x.6622-x4) and amplified by current boosters (Analog Devices Inc. AD811 and Burr-Brown BUF634) before they reached the LEDs. Both the signal generator and current boosters were placed inside the rack shown in the left side of Fig. 4. The RF power and LED arrangements were also configured as per the simulation works described in Sec. 3.2. The receiver, mounted on a movable material buffer station, was composed of an avalanche photo-diode kit (Hamamatsu S8664-50K), an oscilloscope (Tektronix MSO3102), and a laptop. The oscilloscope digitized the received signal, and the laptop performed real-time digital signal processing using LabView; both devices were placed in the bottom of the material buffer station. The positioning results were displayed via a Wi-Fi connection on the monitor placed at the top of the rack. The signal processor not only implemented the algorithm described in Sec. 2.2 but also adopted the Kalman filtering technique applied in our previous research[17] to enhance the positioning performance. The position estimations were calculated in real time at 2 Hz.

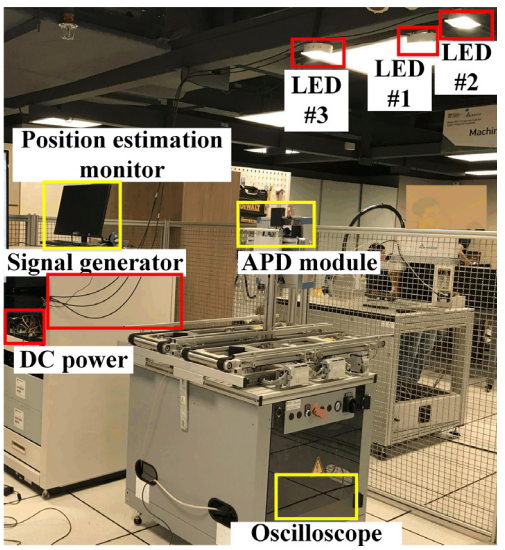

Fig. 4 Experimental setup.

4.2 *Experimental Results and Discussion*

The experiment was performed in a coverage area of 2.2 × 1.8 m^2 in a smart workshop. The height of the APD module was adjusted so that the vertical distance between the transmitters and the receiver could reach 1.4 m. The receiver was mounted on a movable material buffer station, and the positioning performance was validated by tracking the trajectory of the material buffer station moving around underneath the atto-cell VLP unit. The raw POA measurement and interpreted TDOA values after Kalman filtering with calibration at one of the positions to be estimated are shown in Fig. 5. It is evident in Fig. 5(a) that the POA measurements share common fluctuations, which are coincidentally mitigated by the PDOA/TDOA calculation. According to Fig. 5(b), the final TDOA output from the POA measurement is highly stable even though the signal amplitude is as low as 30 mV, indicating the overwhelming accuracy over other methods. It is noteworthy that Figs. 5(a) and 5(b) have different units in Y axis. According to the right side of Eq. (2), 1 deg difference in POA can lead to a difference of around 0.7 ns in time-domain when carrier frequency is 4 MHz. Hence, Fig. 5(b) can be considered as a zoom-in perspective of Fig. 5(a) to show the difference between the measured POAs. In summary, Fig. 5 has clearly presented the high resolution of our scheme in analyzing the gap between the measured POAs. Moreover, the trajectory of the material buffer station was captured during the testing in practical usage, as shown in Fig. 6. Overall, the estimated trajectory is precise except at the edge of the coverage area. Hence, it can be concluded that the accuracy is sufficient to support indoor positioning, tracking, and navigation for AGVs.

A conventional PDOA-based VLP system using a synchronized real local signal was also realized and tested for performance comparison. According to the experimental results, the root mean square of positioning error is 7.37 cm. The positioning error is also concluded in Fig. 7 in CDF format. It can be seen that the positioning error is less than 14 cm with a 90% confidence level. It should be noted that there is a gap between actual and predicted (simulation) performance, especially at the edge of the coverage area. This can be explained by the phase instability and bias measurement error introduced by the practical hardware implementation, which is neglected in our simulations.

As shown in Fig. 7, we further included the performance of the conventional PDOA-based VLP system using real local oscillating signals in the same scenario for comparison.

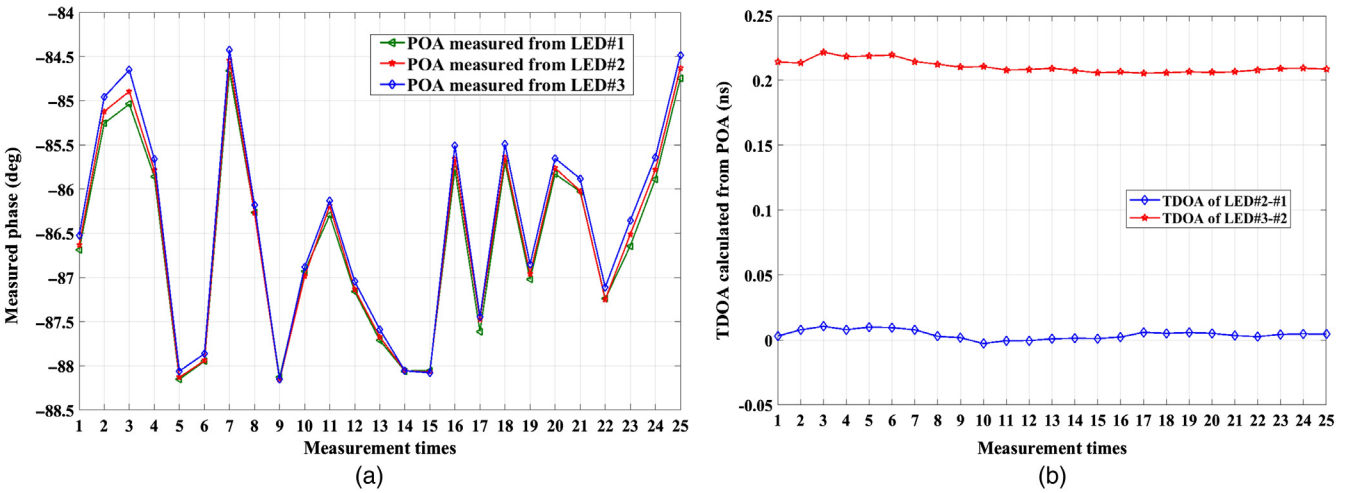

Fig. 5 (a) The raw POA measurement results and (b) TDOA values after Kalman filtering and calibration at (0.4560, −0.4034, 1.4).

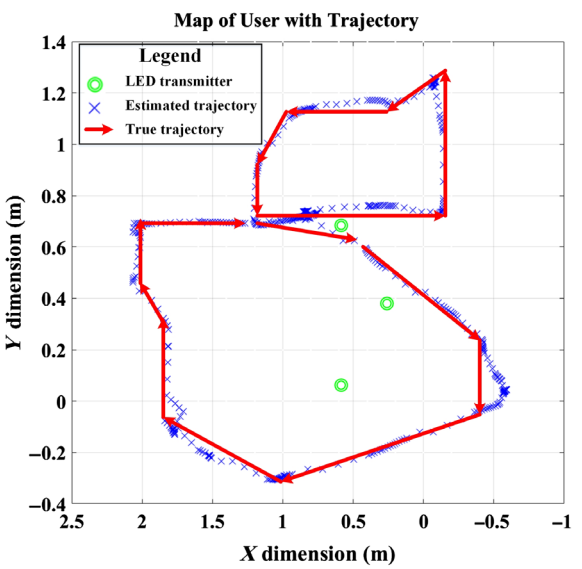

Fig. 6 Real-time trajectory captured in the test.

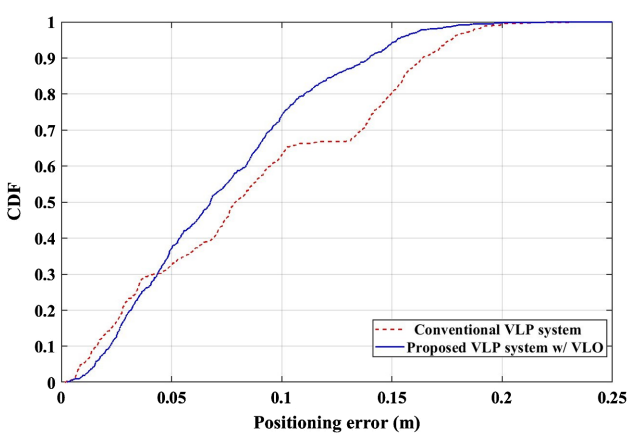

Fig. 7 CDF plot of 2-D positioning error in coverage of 2.2×1.8 m^2.

Evidently, the estimation using a virtual local signal is even better than that using a real local signal. This is likely caused by the way we synchronized the local signal in the experimental setup, where we utilized a cable to broadcast the real local signal. While the receiver was moving, the impedance of the cable broadcasting the real local signal varied slightly with bending and rotation. As a result, there are slightly different initial phase delays at different positions, which is assumed to be consistent at different positions. For this reason, positioning error when using a real local signal becomes larger than that when using virtual local signals. After thorough verification, it can be concluded that the prototype using PDOA with VLO outperforms the conventional PDOA system in terms of both increased accuracy and reduced complexity. Meanwhile, we also compare the result with the work that directly measured TDOA for positioning.[17] Comparing with the results from the previous works,[17] we can summarize that using PDOA scheme can reduce positioning error by 7% than using direct TDOA scheme, as comparable as the accuracy improvement from using VLO. Moreover, it should be noted that directly measuring TDOA needs extremely high time resolution hence excessively high demand for sampling rate of digitization (e.g., $>$200 MSa/s). Therefore, the prototype in this paper that only uses $<$50 MSa/s for sampling has successfully addressed this concern while slightly improving the positioning accuracy.

5 Conclusion

In order to provide a cost-effective indoor positioning and tracking service for AGVs and other important assets in a smart factory, a real-time indoor positioning system using commercially available LED lamps is presented in this paper. The proposed system measures the PDOA of each carrier transmitted from individual modified LED lamps so as to estimate the position of the receiver. The VLO is also applied to reduce the hardware complexity. After carrier frequencies, LED arrangements, and RF power were optimally determined, a prototype atto-cellular positioning system covering 2.2×1.8 m^2 was experimentally demonstrated, and an average positioning accuracy of $\sim$7 cm was achieved. Our

research progress shows great feasibility of applying Li-Fi and VLP technology into scenarios of smart factories and IOT, which can fully enable all the assets and AGVs with location awareness. In the future, the experimental work of cellular VLP network covering the whole shopfloor will be presented. In addition, more techniques to improve positioning accuracy will be further investigated, such as least square algorithm with redundant LED lamps.

Acknowledgments

This work was conducted within the Delta-NTU Corporate Lab for Cyber-Physical Systems with funding support from Delta Electronics Inc. and the National Research Foundation (NRF) Singapore under the Corp Lab@University Scheme. No conflict of interest exits in the submission of this manuscript, and the manuscript is approved by all authors for publication.

References

1. C. Laoudias et al., "A survey of enabling technologies for network localization, tracking, and navigation," *IEEE Commun. Surv. Tutorials* **20**(4), 3607–3644 (2018).
2. L. Angrisani, P. Arpaia, and D. Gatti, "Analysis of localization technologies for indoor environment," in *IEEE 4th Int. Workshop Meas. and Networking (M&N)*, pp. 1–5 (2017).
3. H. Haas et al., "What is LiFi?," *J. Lightwave Technol.* **34**(6), 1533–1544 (2016).
4. D. Tsonev, S. Videv, and H. Haas, "Light fidelity (Li-Fi): towards all-optical networking," *Proc. SPIE* **9007**, 900702 (2014).
5. H. Haas, "LiFi is a paradigm-shifting 5G technology," *Rev. Phys.* **3**, 26–31 (2018).
6. J. Luo, L. Fan, and H. Li, "Indoor positioning systems based on visible light communication: state of the art," *IEEE Commun. Surv. Tutorials* **19**(4), 2871–2893 (2017).
7. Y. Zhuang et al., "A survey of positioning systems using visible LED lights," *IEEE Commun. Surv. Tutorials* **20**(3), 1963–1988 (2018).
8. M. F. Keskin, A. D. Sezer, and S. Gezici, "Localization via visible light systems," *Proc. IEEE* **106**(6), 1063–1088 (2018).
9. H. Zheng et al., "A 3-D high accuracy positioning system based on visible light communication with novel positioning algorithm," *Opt. Commun.* **396**, 160–168 (2017).
10. M. Yasir, S.-W. Ho, and B. N. Vellambi, "Indoor positioning system using visible light and accelerometer," *J. Lightwave Technol.* **32**(19), 3306–3316 (2014).
11. S. Cincotta et al., "High angular resolution visible light positioning using a quadrant photodiode angular diversity aperture receiver (QADA)," *Opt. Express* **26**(7), 9230–9242 (2018).
12. R. Zhang et al., "Image sensor based visible light positioning system with improved positioning algorithm," *IEEE Access* **5**, 6087–6094 (2017).
13. T.-H. Do and M. Yoo, "TDOA-based indoor positioning using visible light," *Photonic Network Commun.* **27**(2), 80–88 (2014).
14. S. Y. Jung, S. Hann, and C. S. Park, "TDOA-based optical wireless indoor localization using led ceiling lamps," *IEEE Trans. Consum. Electron.* **57**(4), 1592–1597 (2011).
15. S. Zhang et al., "PDOA based indoor visible light positioning system without local oscillators in receiver," in *OSA 12th Conf. Lasers and Electro-Opt. Pac. Rim (CLEO-PR)*, pp. 1–3 (2017).
16. A. Naz et al., "PDOA based indoor positioning using visible light communication," *IEEE Access* **6**, 7557–7564 (2018).
17. P. Du et al., "Demonstration of a low-complexity indoor visible light positioning system using an enhanced TDOA scheme," *IEEE Photonics J.* **10**(4), 1–10 (2018).
18. S. Zhang et al., "Robust 3D indoor VLP system based on ANN using hybrid RSS/PDOA," *IEEE Access* **7**, 47769–47780 (2019).
19. S. Zhang et al., "Experimental demonstration of indoor sub-decimeter accuracy VLP system using differential PDOA," *IEEE Photonics Technol. Lett.* **30**(19), 1703–1706 (2018).
20. M. Biagi, S. Pergoloni, and A. M. Vegni, "Last: a framework to localize, access, schedule, and transmit in indoor VLC systems," *J. Lightwave Technol.* **33**(9), 1872–1887 (2015).
21. H. Packard, "GPS and precision timing applications," Application Note 1272 (1996).
22. J. J. Moré, "The Levenberg–Marquardt algorithm: implementation and theory," *Lect. Notes Math.* **630**, 105–116 (1978).
23. M. F. Kazikli and S. Gezici, "Comparative theoretical analysis of distance estimation in visible light positioning systems," *J. Lightwave Technol.* **34**(3), 854–865 (2016).
24. E. Kazikli and S. Gezici, "Hybrid TDOA/RSS based localization for visible light systems," *Digital Signal Process.* **86**, 19–28 (2019).
25. D. Wu et al., "Effect of optimal Lambertian order for cellular indoor optical wireless communication and positioning systems," *Opt. Eng.* **55**(6), 066114 (2016).
26. B. Huang, L. Xie, and Z. Yang, "TDOA-based source localization with distance-dependent noises," *IEEE Trans. Wireless Commun.* **14**(1), 468–480 (2015).
27. M. Gismalla and M. Abdullah, "Performance evaluation of optical attocells configuration in an indoor visible light communication," *Indones. J. Electr. Eng. Comput. Sci.* **14**(2), 668–676 (2019).

Pengfei Du received his B.Eng. degree in mechanical engineering from Sichuan University, Chengdu, China, in 2011, and his PhD degree in optical engineering from Tsinghua University, Beijing, China, in 2016. He is currently a scientist with the A*STAR's Singapore Institute of Manufacturing Technology. His current research interests include Lidar, visible light positioning, Li-Fi, optical IoT, and quantum detection. He is a member of SPIE.

Sheng Zhang received his B.Eng. degree from the School of Optical and Electronic Information, Huazhong University of Science and Technology, China, in 2015. He is currently pursuing his PhD with the School of Electrical and Electronic Engineering (EEE), Nanyang Technological University (NTU), Singapore. His research interests include indoor localization and tracking systems and visible light communication and positioning.

Wen-De Zhong is a professor in the School of Electrical and Electronic Engineering, NTU, Singapore. He received his PhD from the University of Electro-Communications, Japan, in 1993. He joined NTU in 2000 as an associate professor and became a full professor in 2009. His current research interests include visible light communication/positioning, optical fiber communication systems and networks, optical access networks, and signal processing.

Chen Chen received his BS and MEng degrees from the University of Electronic Science and Technology of China, in 2010 and 2013, respectively and his PhD from Nanyang Technological University (NTU), Singapore, in 2017. Currently, he is an assistant professor with the School of Microelectronics and Communication Engineering, Chongqing University, China. His research interests include visible light communications, Li-Fi, visible light positioning, optical access networks, and digital signal processing.

Helin Yang is a PhD candidate in the School of Electrical and Electronic Engineering, Nanyang Technological University, Singapore. He serves as a reviewer for IEEE international journals such as *IEEE Communications Magazine, IEEE Transactions on Wireless Communications*, etc. His current research interests include wireless communication, visible light communication, and resource management.

Arokiaswami Alphones is an associate professor with the School of EEE, NTU. He received his PhD in optically controlled millimeter-wave circuits from the Kyoto Institute of Technology, Kyoto, Japan, in 1992. Since 2001, he has been with the School of Electrical and Electronic Engineering, NTU, Singapore. His current research interests include electromagnetic analysis on planar RF circuits and integrated optics, microwave photonics, metamaterial-based leaky wave antennas, and wireless power transfer technologies.

Ran Zhang received her B.Eng. degree in communication engineering from the Jilin University, China, in 2014 and PhD with the Interdisciplinary Graduate School (IGS), Nanyang Technological University, Singapore in 2019. Her research interests include sensor fusion, indoor localization and tracking system, visible light communication and positioning.